KLOE Memo 250 October 2001

Analysis of $\eta\pi^0\gamma$ with $\eta \rightarrow \pi^+\pi^-\pi^0$.

C.Bini, D.Leone

Universitá "La Sapienza" and INFN Roma

Abstract

The branching ratio of $\phi \rightarrow \eta\pi^0\gamma$ is measured using the $\eta \rightarrow \pi^+\pi^-\pi^0$ decay. The invariant mass spectrum of the $\eta\pi^0$ system is also obtained. The $\rho^0\pi^0$ and $\omega\pi^0$ contributions are subtracted in order to evaluate the $\phi \rightarrow a_0\gamma$ branching ratio and spectrum.

1 Introduction.

The analysis of $\eta\pi^0\gamma$ allows to study the decay $\phi \rightarrow a_0^0\gamma$. The $a_0(980)$ state is interpreted as the lowest mass isospin 1 scalar meson, mostly decaying in $\eta\pi^0$. The branching ratio $\phi \rightarrow a_0^0\gamma$ that can be extracted from the rate of events, and the invariant mass spectrum of the $\eta\pi^0$ system are of special interest in the assessment of the nature of this scalar meson, and allows to compare models based on different approaches [1]-[7].

Depending on the η decay mode, $\eta\pi^0\gamma$ results in different final states. Tab.1 shows the possible final states with their probabilities [1] . The number of events per pb^{-1} in KLOE at the ϕ resonance peak is shown for each final state assuming a peak cross-section of 3.3 μb and BR($\phi \rightarrow \eta\pi^0\gamma$)=$8\times10^{-5}$ [2] . $\eta\pi^0\gamma$

[1] π^0 decays in $\gamma\gamma$ apart form a 1.2% decay in $e^+e^-\gamma$ (the other observed decay channels are below 10^{-4}). The values given in Tab.1 refer to the main $\pi^0 \rightarrow \gamma\gamma$ final state only. Decays with two tracks in place of a photon should be considered for each final state with probabilities reduced by a factor about 100.

[2] Measurements of these quantity are from VEPP-2M[8,9]: $(8.8 \pm 1.4 \pm 0.9) \times 10^{-5}$ (SND) and $(9.0 \pm 2.4 \pm 1.0) \times 10^{-5}$ (CMD-2). A preliminary result from KLOE is[10]

Table 1
Possible final states (η branching ratios are taken from PDG 2000).

η decay mode	BR($\eta \to X$)	final state	Events /pb^{-1}
$\gamma\gamma$	0.3933±0.0025	5 photons	105
$\pi^0\pi^0\pi^0$	0.3224±0.0029	9 photons	85
$\pi^+\pi^-\pi^0$	0.230±0.004	2 tracks + 5 photons	60
$\pi^+\pi^-\gamma$	0.0475±0.0011	2 tracks + 4 photons	13
$e^+e^-\gamma$	$(4.9\pm1.1)\times10^{-3}$	2 tracks + 4 photons	1
$\pi^0\gamma\gamma$	$(7.1\pm1.4)\times10^{-4}$	7 photons	0.2
$\mu^+\mu^-\gamma$	$(3.1\pm0.4)\times10^{-4}$	2 tracks + 4 photons	0.1

can be observed in fully neutral final states (5 photons, 9 photons, 7 photons) and charged/neutral final states (2 tracks + 5 photons, 2 tracks + 4 photons).

The analysis of the most frequent final state, namely the 5 photons, is presented in ref.[10]. In this memo we present the results obtained from 2 tracks + 5 photons final states. We notice that, due to the completely different backgrounds and systematic conditions of this final states respect to the 5 photons one, the comparison between the two results is very relevant.

Furthermore we stress that the analysis of this decay chain has never been done before by any experiment.

2 Event selection strategy.

A final state with 2 tracks coming from the interaction region and 5 prompt photons is in principle a unique signature of $\eta\pi^0\gamma$ with $\eta \to \pi^+\pi^-\pi^0$. Infact no other decay chain gives the same final state[3]. Unfortunately a selection uniquely based on the request of 2 "tracks" and 5 "photons" is not possible. Infact the presence of other final states with "similar" topologies and larger expected rates as shown in table.2 makes the "photon counting" the critical selection step. On the other hand the "photon counting" is known to suffer from cluster splitting and merging, from photon losses for acceptance and efficiency and finally for the presence of unwanted accidental clusters superimposed to the event. Furthermore wrong assignments of clusters to tracks

$(7.4 \pm 0.5) \times 10^{-5}$

[3] $K_S \to \pi^+\pi^-\gamma$ and $K_L \to \pi^0\pi^0$ prompt or the one obtained changing K_S and K_L give final states with 2 tracks + 5 photons with equivalent BR around or below 10^{-7}.

Table 2
Main sources of background to the 2 tracks + 5 photons final states. For $\omega\pi^0$ that is dominated by non-resonant contribution, the number of events is evaluated using the cross section at the ϕ peak of $8.25 \pm 0.14 \pm 0.43$ nb according to ref.[11].For $K_S K_L$ only K_L decays within ~10 cm are considered as possible background to prompt decay events.

	Decay mode	final state	Events /pb^{-1}
1	$\omega\pi^0 : \omega \to \pi^+\pi^-\pi^0$	2 tracks + 4 photons	7300
2	$\eta\gamma : \eta \to \pi^+\pi^-\pi^0$	2 tracks + 3 photons	11500
3	$K_S K_L$: $K_S \to \pi^+\pi^-$ / $K_L \to \pi^0\pi^0\pi^0$ "prompt"	2 tracks + 6 photons	~4600
4	$K_S K_L$: $K_S \to \pi^0\pi^0$ / $K_L \to \pi^+\pi^-\pi^0$ "prompt"	2 tracks + 6 photons	~1200
5	$K_S K_L$: $K_S \to \pi^0\pi^0$ / $K_L \to \pi l \nu$ "prompt"	2 tracks + 4 photons	~6000

can also contribute to a bad reconstruction of the final state topology.

For these reasons a selection strategy based on kinematical fits has been developed. The strategy is the same adopted for other final state selections [10,12]. The only significant difference is that the kinematical fits are done in a numerical way using MINUIT [4].

The event selection proceeds in the following steps:

(1) Events are taken from the RAD stream [13].
(2) Are accepted events with two tracks from the interaction region + 5 "prompt" neutral clusters with $\theta > 21^o$ (θ being the photon angle respect to the z axis) and E >10 MeV. A "prompt" neutral cluster is a non associated cluster with a $t - R/c$ value at 0 within 5 times the time resolution at that energy. In the photon counting the cluster algorithm with splitting recovery [14] has been used. Also the function "timesmooth2000" has been used to remove the bias on timing due to photon energy and position.
(3) Cuts are done on total energy and momentum: $900 < E_{tot} < 1160$ MeV $|\mathbf{P_{tot}}| < 110$ MeV/c, and in the scalar sum of track momenta $|\mathbf{P_1}|+|\mathbf{P_2}| <$ 420 MeV.
(4) Kinematical fit 1: only energy-momentum conservation and speed of light for the photons, no mass constraints; the number of degrees of freedom is equal to the number of constraints: 4(energy-momentum) + 5(speed of photons) = 9. A cut on the χ^2 probability [5] is done p(χ^2_1) > 2%.

[4] MINUIT has been used in fortran-callable mode, by a stand-alone fortran program that reads prod2ntu ntuples.
[5] In the definition of this and of the other χ^2, the σ are taken differently for data

(5) Using the values of energies, momenta, times and positions from kinematical fit 1, 30 combinations are build, corresponding to the 30 ways with which one can associate tracks and clusters in such a way to obtain $\eta\pi^0\gamma$ final states [6]. A combination χ^2, χ^2_{comb} is defined with 3 degrees of freedom:

$$\chi^2_{comb} = \frac{(M_{\pi^0_1} - M_{\pi^0})^2}{\sigma^2(M_{\pi^0})} + \frac{(M_{\pi^0_2} - M_{\pi^0})^2}{\sigma^2(M_{\pi^0})} + \frac{(M_{\pi^+\pi^-\pi^0} - M_\eta)^2}{\sigma^2(M_\eta)}$$

where $\sigma(M_{\pi^0})$ and $\sigma^2(M_\eta)$ are obtained by the width of the peaks in the relevant distributions. Combinations with $p(\chi^2_{comb}) > 2\%$ are considered good. All the others are rejected.

(6) Kinematical fit 2 on all the combinations selected by previuos step: mass constraints according to the assignment hypothesys of the combination are added to the Kinematical Fit 1. The number of degrees of freedom is now 12. If there is at least one combination with $p(\chi^2_2) > 2\%$ the event is selected. The combination with the best $p(\chi^2_2)$ is considered the good one [7]

(7) Events where the radiative photon energy E_{rad} is below 20 MeV are discarded. This is to remove events with a spurious low energy cluster that the fit itself tries to remove. A significant amount of such events is observed and can be attributed to background 1.

3 Montecarlo studies of efficiency for signal and background events.

Simulated signal and background events have been used to evaluate efficiency and background contamination. Two streams are in use for $\eta\pi^0\gamma$: one generated making an assumption for the $\eta\pi^0$ invariant mass spectrum based on one of the a_0 models [15]; another one assuming pure phase-space $\eta\pi^0\gamma$ production with a dumping factor to make almost uniform the E_{rad} spectrum.

In all the Montecarlo events used accidental clusters have been added using the procedure described in [16]

Two corrections have been applied to the Montecarlo for this efficiency evaluation:

---

and for Montecarlo, according to the best evaluations.

[6] There are 15 possibilities to get 2 π^0s out of 5 photons. For each of them there are 2 choices in the association of one π^0 to the $\pi^+\pi^-$ pair. 15×2=30 combinations.

[7] In case of more than one good combination the choice of the one with larger $p(\chi^2_2)$ seems the best choice (different formulations have been tried on Montecarlo).

- ratio between photon detection efficiency evaluated by data and by Montecarlo. This efficiency ratio has been evaluated by $e^+e^-\gamma$ and $\pi^+\pi^-\pi^0$ control samples [17,18]. The overall effect when folded with the expected photon energy distribution is an efficiency reduction of $\sim 4\%$ consistent within 1 % using the two samples.
- ratio between tracking efficiencies evaluated by data and by Montecarlo. The control samples is [18] is provided by $K_S \to \pi^+\pi^-$ events tagged by a K_L interacting in the calorimeter (Kcrash). The effect is a further 5 % reduction of the efficiency.
- ratio between vertex efficiency evaluated by data and by Montecarlo. The control sample is provided by prompt $K_L \to \pi e \nu$ tagged by $K_S \to \pi^0\pi^0$ as described in [19]. The momentum spectra of the two pions of $\eta\pi^0\gamma$ is very close to the one π and e in the control sample. The overall estimated efficiency is (97.9$\pm$ 1.5)%.

Since the $\eta\pi^0$ invariant mass is the most relevant kinematical variable in the analysis, the efficiency has been evaluated as a function of this variable using the phase-space based simulation. Fig.1 shows the efficiency as a function of M($\eta\pi^0$). It turns out to be about 19% and almost uniform over the full range.

The uncertainty on this efficiency evaluation includes the statistics of the Montecarlo sample (contributions of 1.8%) and the uncertainties due to the photons (1%), tracks and vertex efficiency corrections (2% each). The total uncertainty is 3.6%.

Table.3 shows the overall efficiency and selection probabilities for signal and background final states together with the number of expected events for a 16 pb^{-1} sample. The most relevant background contribution comes from category 1. In any case the number of expected events is such that the contribution of the background subtraction to the uncertainty is negligible at the present statistical level. For larger data samples, a larger Montecarlo statistics is required.

The resolution on the variable M($\eta\pi^0$) is evaluated comparing the reconstructed values of M($\eta\pi^0$) to the true values. The result is shown in Fig.2: a resolution of 3.8 MeV on most of the spectrum is obtained. The non-gaussian tails are due to events where a misassignment of the radiative photon is done. The amount events more than 3 sigma out of 0 is 11.7%.

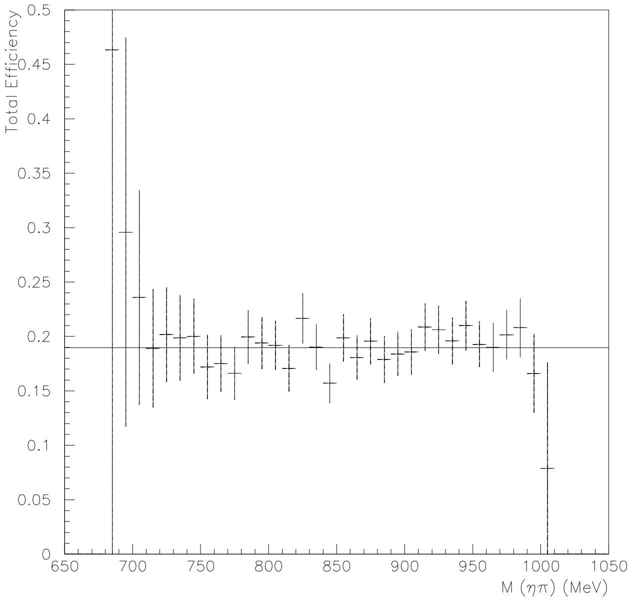

Fig. 1. Efficiency as a function of M($\eta\pi^0$).

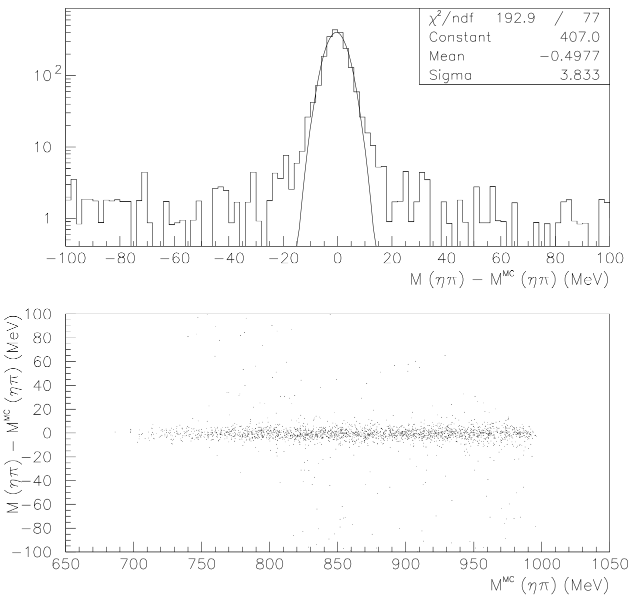

Fig. 2. Distribution of the difference between reconstructed M($\eta\pi^0$) and true value. Gaussian fit giving the resolution (upper plot) and difference vs. M($\eta\pi^0$) (lower plot) showing no significant dependence on the value of M($\eta\pi^0$).

Table 3
Effect of the selection procedure on Montecarlo samples corresponding to signal and background events. The expected number of events for a 16 pb−1 sample is shown. Upper limits are at 90% C.L..

final state	selected events	expected events / 16 pb^{-1}
$\eta\pi^0\gamma$	19.0%	190
back 1	1/33000	3.6
back 2	0/95000	<4
back 3	0/83000	<2
back 4-5	0/92000	<2

Table 4
Number of surviving events for the 16 pb^{-1} sample at each selection stage. The effect of the selection on the Montecarlo sample is also shown.

Cut	data	Montecarlo
generated		11763
triggered		11628
Ev.Cl.(RAD substream 3)	38408	6482
2T + 5 photons	7121	3112
E_{tot} - $\|P_{tot}\|$	4331	2976
kinematical fit 1	1967	2714
combination	1386	2649
kinematical fit 2	201	2247
E_{rad} > 20 MeV	197	2240

4 Data reduction.

Table 4 shows the number of events at every selection stage for the full sample of 2000 data (the 16 pb^{-1} sample) together with the same numbers for the Montecarlo events.

The starting sample consists of events with 2 tracks from the interaction region + 5 photons (third row in table.4). For these events the distribution of E_{tot} and $|\mathbf{P_{tot}}|$ is shown in Fig.3. The cut is also indicated. Events out of the cut are mostly events with missing energy and momentum.

After the kinematical fit 1 the distributions of "η" and "π^0" invariant masses for all the combinations are shown in Fig.4. In the η plot a small peak at the η

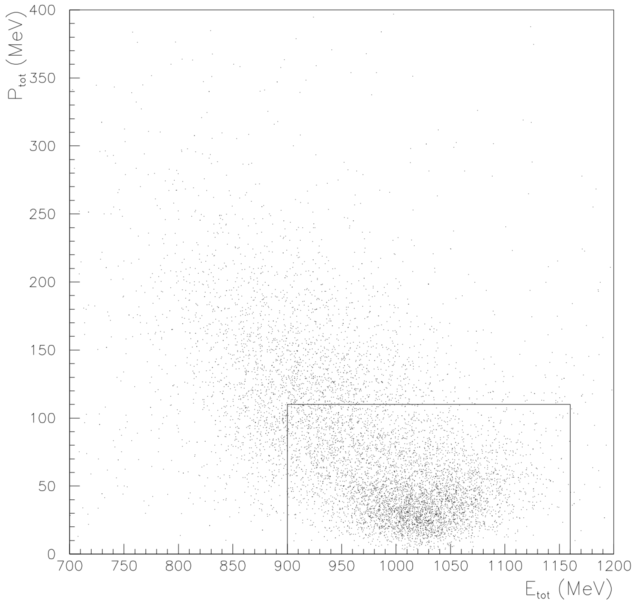

Fig. 3. Scatter plot of $|\mathbf{P_{tot}}|$ vs E_{tot} for a sample of events before any kinematical fit. The box corresponds to the cut.

mass is observed together with a slightly more consistent peak at the ω mass. We can argue that at this stage of the analysis the sample contains residual $\omega\pi^0$ events (2 tracks + 4 photons, back-1 according to previous tables) with a spurius cluster that simulates a photon. On the other hand, $\eta\pi^0\gamma$ events give rise to η peak. A rough estimate of the excess of events in the η peak gives $\sim$ 150 events out of the 2000 events surviving at this stage. No clear structure is observed at the neutral kaon mass, indicating a negligible amount of background 4.

After the kinematical fit 2 the mass constraints have removed the ω peak (see Fig.5) and most of the background. The distribution is in nice agreement with the same distribution for Montecarlo $\eta\pi^0\gamma$ events.

The last cut ($E_{rad} > 20$ MeV) rejects 4 events. If not applied we expect 7 more background events coming from background 1 (3/33000 instead of 1/33000 in Tab.3) in rough agreement with the 4 observed.

5 Results on 2000 data (~ 16 pb^{-1}).

The analysis has been applied on the RAD stream of the data taken in 2000, from run 15174 to 17330, corresponding to an integrated luminosity of 16.33 pb^{-1}. The integrated luminosity is evaluated using very large angle Bhabha

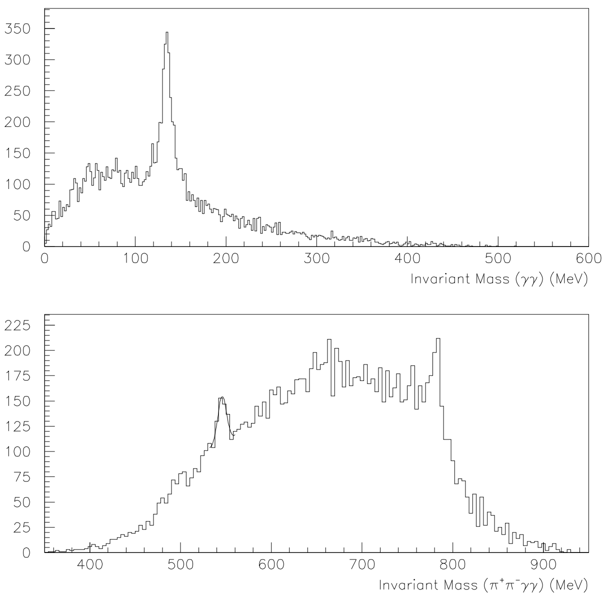

Fig. 4. Distribution of the invariant mass of all the pairs of photons (upper plot) and of the 2 tracks + 2 photons (lower plot). Distributions are for the events surviving kinematical fit 1 without mass constraints. For every event there are 10 possibile choices of a π^0, and so 10 entries in each plot.

(vlab see [20]) counting the sum of luminosities for the runs in the sample. The overall uncertainty is $\pm 1\%$.

In the data production the calorimeter part has been reconstructed, in such a way to use the correct calibration.

The final number of selected events is 197. Fig.6 shows the M($\eta\pi^0$) invariant mass spectrum obtained. In Fig.7 the distribution is compared with the expected pure phase-space distribution. In the same figure the 197 events are shown in a Dalitz diagram $M(\eta\pi^0)$-$M(\eta\gamma)$. The curve superimposed to the data in the lower plot corresponds to uniform population within the contour of the Dalitz diagram.

In order to extract the $a_0(980)$ contribution, other two possible decay chains contributing to the $\eta\pi^0\gamma$ final state have been considered:

- B(ρ): $\phi \to \rho^0\pi^0$ with $\rho^0 \to \eta\gamma$;
- B(ω): $e^+e^- \to \omega\pi^0$ with $\omega \to \eta\gamma$;

The amount of these events has been obtained using the cross-sections and BRs from PDG and from more recent data [8] from VEPP-2M [21,22] and taking

[8] For BR($\rho \to \eta\gamma$) the weighted average of the two Novosibirsk experiments[21,22]

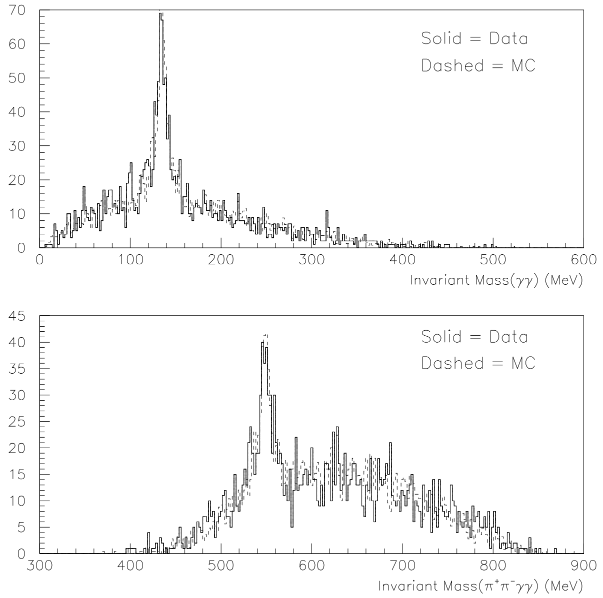

Fig. 5. Distribution of the invariant mass of all the pairs of photons (upper plot) and of the 2 tracks + 2 photons (lower plot) for the 197 final candidates. For every event there are 10 possibile choices of a π^0, and so 10 entries in each plot. The variables are evaluated using the output of kinematical fit 1.

into account the KLOE selection probability; their expected distributions in $M(\eta\pi^0)$ is obtained using the KLOE Montecarlo taking into account ρ^0 and ω line shapes. No interference term between $\rho\pi$ and $a_0\gamma$ has been considered (for a detailed discussion of this point see [23]). Fig.8 shows the expected contribution of $B(\rho)$ and of $B(\omega)$ superimposed to the KLOE spectrum. It can be seen that the two contributions (essentially $B(\rho)$) describe well the low $M(\eta\pi^0)$ part of the spectrum. A subtraction allows in principle to obtain the "a_0^0" spectrum shown in the lower plot of the same Fig.8.

Two branching ratios have been evaluated.

- $BR(\phi \to \eta\pi^0\gamma)$ has been evaluated subtracting to the N=197 events only the background due to different final states B=3.6 (as shown in Table.3)

has been used.

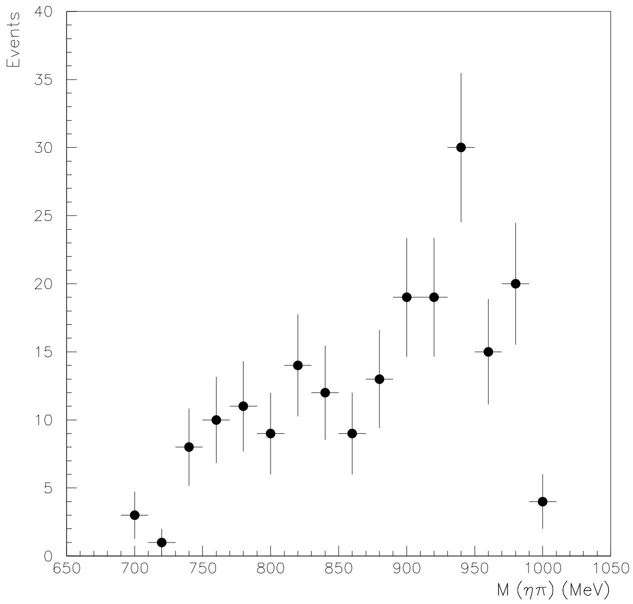

Fig. 6. Distribution of the invariant mass M($\eta\pi^0$) of the $\eta\pi^0$ for the final sample of 197 events.

and normalizing according to the:

$$BR(\phi \to \eta\pi^0\gamma) = \frac{N - B}{\epsilon_{tot} \times BR(\eta \to \pi^+\pi^-\pi^0)} \frac{1}{\sigma_\phi \times L_{int}}$$

where ϵ_{tot} is the efficiency, σ_ϕ is the ϕ production cross-section [9] and $L_{int} =$ 16.33 pb^{-1} is the integrated luminosity. We obtain:

$$BR(\phi \to \eta\pi^0\gamma) = (8.19 \pm 0.60_{stat} \pm 0.15_{bck} \pm 0.50_{syst}) \times 10^{-5}$$

. The systematical uncertainty comes from:
· (1.7 %) the knowledge of $BR(\eta \to \pi^+\pi^-\pi^0)$;
· (4.2 %) due to σ_ϕ;
· (1.0 %) quoted uncertainty on the luminosity;
· (3.6 %) from the accuracy of efficiency evaluation due to Montecarlo statistic (1.8 %) and to systematics in the corrections based on data (3.2%).
The contribution of the background subtraction is negligible. % uncertainty on the value .

[9] The cross-section is obtained from $\phi \to \eta\gamma \to \pi^0\pi^0\pi^0\gamma$ events [25]: $\sigma_\phi = 3.30 \pm 0.01 \pm 0.14 \mu b$. The result nicely agrees with $\sigma_\phi = 3.37$ obtained applying the same analysis on $\phi \to \eta\gamma$ with $\eta \to \gamma\gamma$. We notice that the result obtained in ref.[26] is lower by ∼7% due to a loss of events in the event classification program originated by background in the drift chamber.

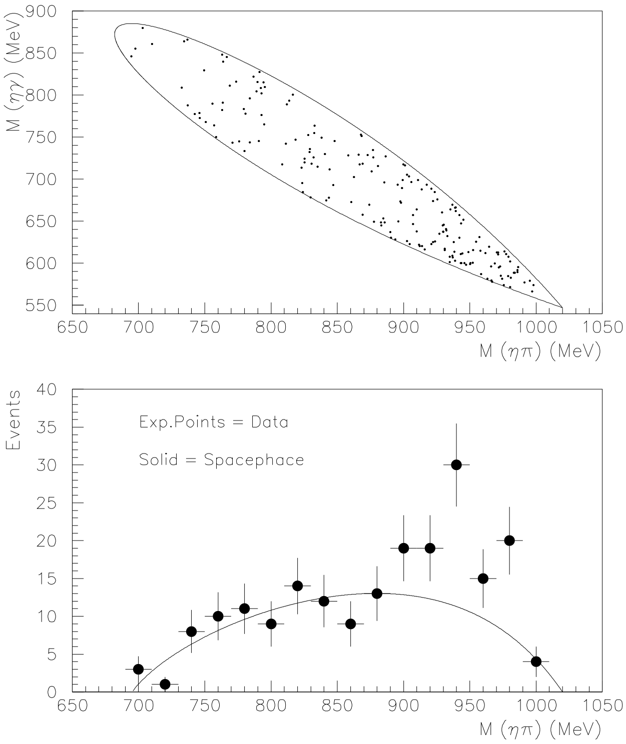

Fig. 7. (Upper plot): Dalitz diagram M($\eta\pi^0$) - M($\eta\gamma$) with allowed phase-space contour; (Lower plot): M($\eta\pi^0$) distribution compared with pure phase-space.

- BR($\phi \to a_0^0\gamma$) has been evaluated subtracting also the estimated number of $\eta\pi^0\gamma$ events coming from B(ρ) and B(ω) decay chains. The number of events from these decay chains has been estimated as follows:

  $$B(\rho) = \sigma_\phi \times L_{int} \times BR(\phi \to \rho\pi) \times \frac{1}{3} \times BR(\rho^0 \to \eta\gamma) \times BR(\eta \to \pi^+\pi^-\pi^0) \times \epsilon_{tot} = 36 \pm 4$$

  $$B(\omega) = \sigma(e^+e^- \to \omega\pi^0) \times L_{int} \times BR(\omega \to \eta\gamma) \times BR(\eta \to \pi^+\pi^-\pi^0) \times \epsilon_{tot} = 2.8 \pm 0.3$$

  where ϵ_{tot} is essentially the same as for the a_0^0 events (see Fig.1).
  After the subtraction we obtain:

  $$BR(\phi \to a_0^0\gamma) = (6.55 \pm 0.59_{stat} \pm 0.35_{bck} \pm 0.40_{syst}) \times 10^{-5}$$

  where the systematic uncertainty is due to the same reasons quoted for the previous branching ratio. The significant contribution coming from the background subtraction is dominated by the statistical fluctuation of the 39 estimated background events.

Fig.9 compares the $\eta\pi^0$ spectrum obtained in this analysis with the same spectrum obtained by the 5 photon analysis with and without background subtraction. A good agreement is observed. The comparison is done by normalizing

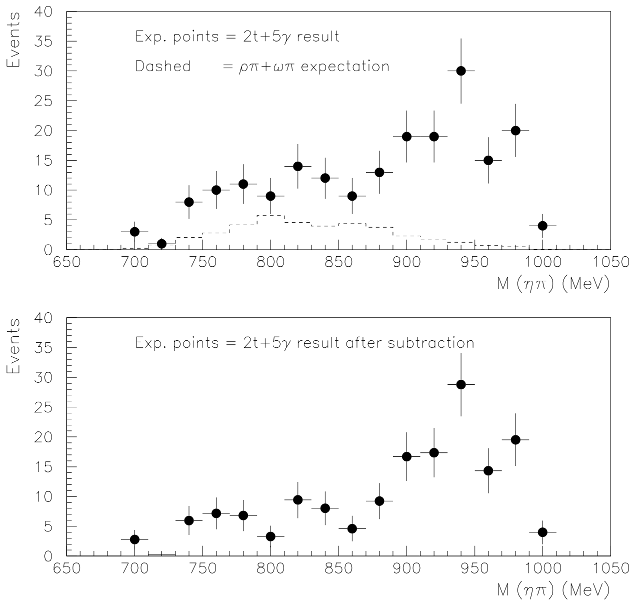

Fig. 8. (Upper plot):$\eta\pi^0$ invariant mass spectrum compared with the sum of the expected contributions from the two backgrounds B(ρ) and B(ω). The background distribution is normalized in such a way that the area is equal to the expected number of events from these two channels. (Lower plot): the same distribution after subtraction of B(ρ) and B(ω) backgrounds. It is "in principle" a spectrum of a_0^0.

to the same number of events. We notice also that since the efficiency curves are rather different in the two analysis, they have to be taken into account in the fit to the distributions.

Finally in fig.10 the distribution of the cosine of the angle of the radiative photon respect to the beam direction is shown and compared with the Montecarlo distribution. The position of the radiative photon is taken by the output of the second kinematic fit. The $\alpha(1+cos^2\theta_\gamma)$ is well reproduced and the acceptance cut for $cos\theta_\gamma$ larger than 0.9 is consistent for data and Montecarlo.

6 Comparison of the final sample with the Montecarlo sample.

Since the efficiency evaluation relies mostly on Montecarlo, the final data sample of 197 events has been compared with a Montecarlo sample obtained applying the same selection procedure of the data. The Montecarlo used is the one assuming pure phase-space $\eta\pi^0\gamma$ production because the kinematics turns out to represent better the observed final spectrum. Fig.11 shows a data vs MC comparison of (p_T,θ_t) distributions for tracks and (E_γ, θ_γ) for photons. The agreement is rather good at the present level of statistical accuracy of

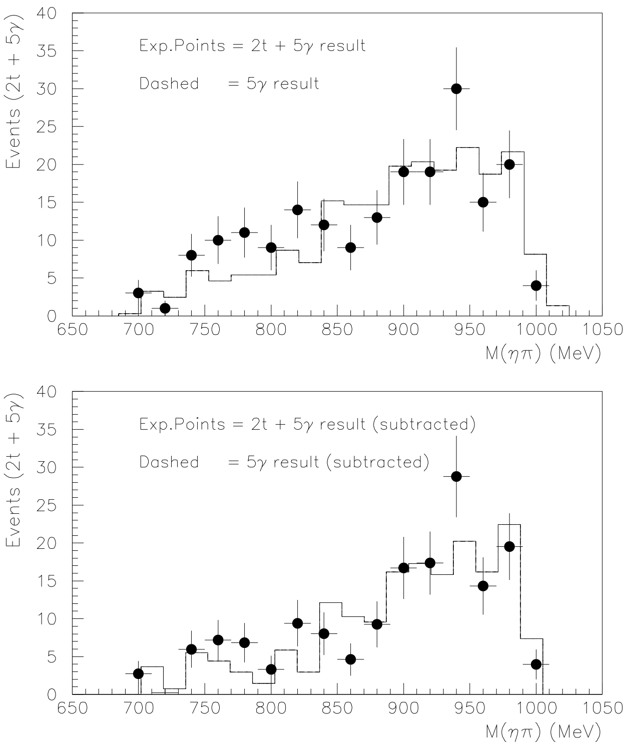

Fig. 9. Comparison between the $\eta\pi^0$ invariant mass spectrum obtained by KLOE using $\eta \to \gamma\gamma$ (histogram [24]) and $\eta \to \pi^+\pi^-\pi^0$ (points, the result of this analysis). (Upper plot) spectra without subtraction, (lower plot) spectra after subtraction. The distributions are normalized to the same number of events.

this sample.

The selection of 2 tracks + 5 photons final states, is based on photon counting in events with 2 low momentum charged tracks. Some critical points on photon counting have been investigated and checked with Montecarlo.

- The first critical point in the photon counting is the width of the time window. The stability of the result respect to this parameter is shown in Fig.12 for data and Montecarlo. The cut at 5σ turns out to be well within a stability plateau.
- Track-cluster association is also used in the photon counting. Fig.12 shows the number of associated tracks per event for data and Montecarlo. Due to the low values of the track momenta, the probability for a track to be associated with a cluster is low. The low probability for both tracks to be associated does not allow to require that both pion tracks are associated in the selection procedure. Again data and Montecarlo reasonably agree.
- Finally the effect of the recovery splitting procedure on data and Montecarlo is shown in Tab.5. No significant discrepancy is observed. The loss of 4 events

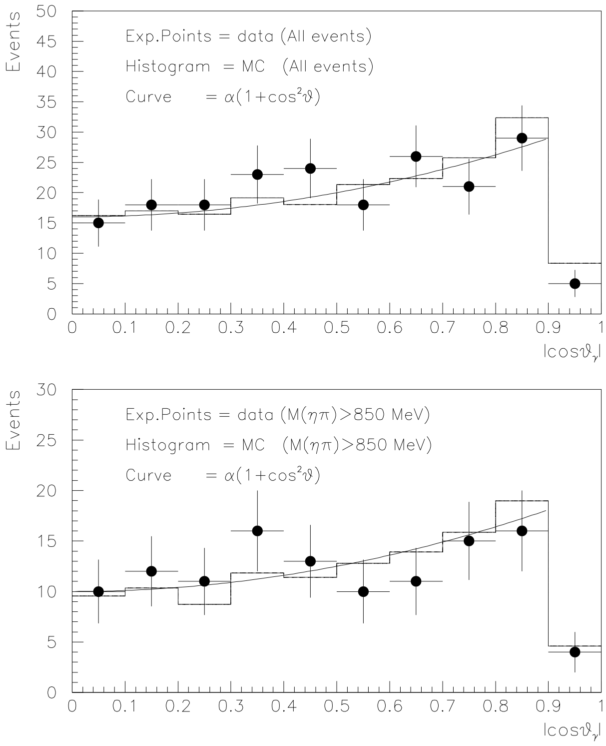

Fig. 10. Distribution of the polar angle of emission of the radiative photon for the final selected sample (exp.points) compared to the Montecarlo normalized to the same number of events (histogram) and to the $\alpha(1 + cos^2\theta_\gamma)$ curve.(Upper plot) all event are included (Lower plot) only the events with M($\eta\pi$) larger than 850 MeV in order to select the a_0 part of the spectrum.

Table 5
Comparison of the effect of the recovery splitting on data and Montecarlo samples. Percentage are taken respect to N_2.

	data	MC
N_1 (without recovery splitting)	172 (.87)	2093 (.83)
N_2 (after recovery splitting)	197	2517
ΔN_1 (recovered)	29 (.15)	427 (.17)
ΔN_2 (lost)	4 (.02)	3 (.001)

in the data sample (larger than expected), can be attributed to the loss of residual background events not present in the Montecarlo sample.

Fig.13 shows the distribution of the χ^2 probabilities of the first and of the second kinematical fits for the final data sample and the Montecarlo sample. In both distributions the cut is applied at $p = 0.02$. Possible differences between

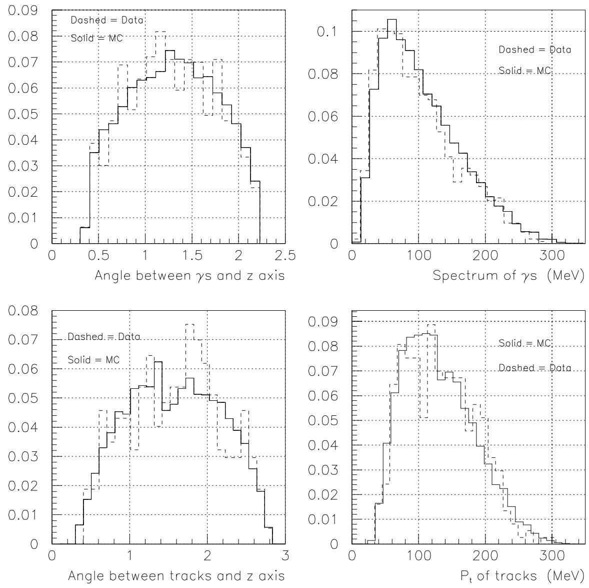

Fig. 11. Comparison between tracks and photons in the final data sample and in the Montecarlo selected sample. The variables plotted are p_T, θ_t, E_γ and θ_γ.

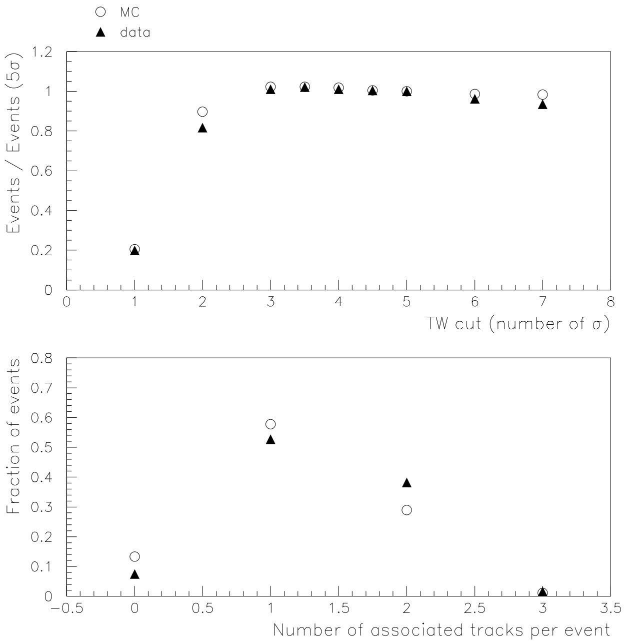

Fig. 12. Number of selected events as a function of the width of the time window used to count the photons for data and Montecarlo (upper plot); distribution of the number of associated tracks: 3 corresponds to larger than 2 (1 of the two tracks associated with more than one cluster) (lower plot).

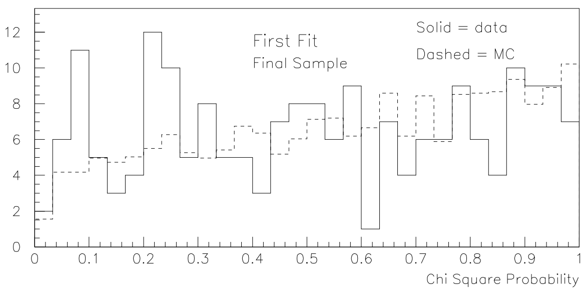

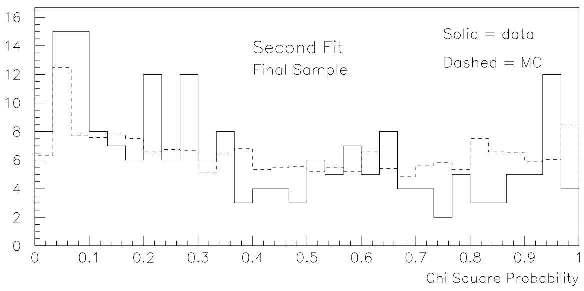

Fig. 13. Distribution of the χ^2 probability for the first and the second kinematical fit. The final sample of data is compared with Montecarlo.

data and Montecarlo in the slopes respect to the uniform behaviour depend on a not correct assessment of the normalization in the χ^2 definition and affect the efficiency evaluation. From the plots we estimate a systematic due to these cuts well below 1%.

7 Conclusion

From the analysis presented in this memo, the branching ratio of $\phi \to \eta\pi^0\gamma$ is obtained together with a 197 events spectrum of the $\eta\pi^0$ invariant mass. By subtracting the known contributions from $\rho\pi$ and $\omega\pi$ final states a branching ratio is also guessed for the a_0^0 radiative production. The residual background turns out to be negligible at the present statistical level, and the final sample shows a convincing agreement with the Montecarlo sample.

A comparison of the obtained spectrum with different models will be described in a forthcoming memo.

References

[1] R.L.Jaffe, Phys.Rev. D15 (1977) 15;

[2] J.Weinstein, N.Isgur, Phys.Rev.Lett. 48,10 (1982) 659;

[3] F.E.Close et al., Phys.Lett. B319 (1993) 291;

[4] F.E.Close, N.Isgur, S.Kumano, Nucl.Phys. B389 (1993) 513;

[5] E.Marco et al., Phys.Lett. B470 (1999) 20;

[6] A.Bramon et al., Phys.Lett. B494 (2000) 1;

[7] M.Alford, R.L.Jaffe, Nucl.Phys. B578 (2000) 367;

[8] M.N.Achasov et al., Phys.Lett. B479 (2000) 53;

[9] R.R.Akhmetshin et al., Phys.Lett. B462 (1999) 380;

[10] P.Gauzzi, "Analysis of $\phi \to \eta\pi^0\gamma$ with $\eta \to \gamma\gamma$" KLOE Memo 01-247 June 2001;

[11] V.M.Aulchenko et al, JETP 90 (2000) 927;

[12] S.Giovannella, S.Miscetti, "Status of the $\phi \to f_0\gamma \to \pi^0\pi^0\gamma$ analysis" KLOE Memo 244 May 2001;

[13] C.Bini, P.Gauzzi, "Event classification of non-K phi decays" KLOE Memo 171 December 1998;

[14] A preliminary version of the recovery splitting function has been provided by S.Miscetti;

[15] A.Ferrari et al., "A generator for the $\phi \to f_0(980)\gamma \to \pi\pi\gamma$ process: description and guide for GEANFI users" KLOE Memo 243 May 2001;

[16] S.Miscetti, T.Spadaro, "Rate measurement of accidental clusters in the EMC" KLOE Memo 251 Oct 2001;

[17] G.Cabibbo, tesi di dottorato, Universitá "La Sapienza" 2000;

[18] T.Spadaro, private comunication and forthcoming tesi di dottorato, Universitá "La Sapienza" 2001;

[19] T.Spadaro, C.Gatti, "Measurement of $BR(K_S \to \pi e\nu)$" KLOE Memo in preparation;

[20] A.Denig, private comunication;

[21] M.N.Achasov et al., JETP 72,6 (2000) 282;

[22] R.R.Akhmetshin et al., Phys.Lett. B509 (2001) 217;

[23] N.N.Achasov, E.Gubin, Phys. Rev. D63 (2001) 094007;

[24] The spectrum shown is an updated version of the spectrum shown in Ref.[10] provided us by P.Gauzzi.

[25] Analysis presented by S.Miscetti, memo in progress;

[26] F.Scuri, "Study of the ϕ decays detected by three neutral cluster final state" KLOE Memo 217 September 2000;